Journal of Applied Electrochemistry (2005) 35:675–681
DOI 10.1007/s10800-005-1389-1

A fluidized bed photoreactor exploiting a supported photocatalyst with adsorption pre-concentration capacity

E. VAISMAN[1], M. F. KABIR[2], A. KANTZAS[2] and C. H. LANGFORD[1,*]
[1]*Department of Chemistry, University of Calgary, 2500 University Dr., NW, Calgary, Alberta, Canada T2N 1N4*
[2]*Department of Chemical and Petroleum Engineering, University of Calgary, 2500 University Dr., NW, Calgary, Alberta, Canada T2N 1N4*
*(*author for correspondence, e-mail: chlangfo@ucalgary.ca; phone: +1-403-220-3228; fax: +1-403 289-9488)*

Received 30 June 2004; accepted in revised form 14 December 2004

Key words: adsorbent, catalyst support, fluidized bed, photocatalyst, photocatalytic, reactor, titanium dioxide, zeolite

Abstract

Laboratory and small pilot scale fluidized bed photoreactors are described that utilize an integrated photocatalyst adsorbent (IPCA) mounted on porous silica beads as support protecting against IPCA attrition. The active material is Degussa P-25 TiO_2 bound to a Silicalite I zeolite adsorbent. Operating conditions for fluidization that achieves uniform illumination of photoactive particles are determined. Axial and multi-lamp configurations are compared. The small pilot reactor is calibrated against the laboratory reactor. Sub-stoichiometric acceleration of phenol oxidation by H_2O_2 was observed.

1. Introduction

A photocatalytic process must be constructed from three elements; a reactor, a light source, and a photocatalyst. In our work, we have focused on heterogeneous photocatalysts that are integrated with adsorbents to offer opportunities for pre-concentration [1–3]. Optimal state of the art lamps were not available. Only the requirements of matching the output to the actinic spectrum of the photocatalyst and measuring intensities in the reactor were met. This is a major limitation on the quantitative significance of the results reported and a consequence of limited electrical infrastructure. However, our interest in integrated heterogeneous photocatalysts presents us with major challenges for complementarity of catalyst and reactor design. The present paper reports on a reactor design to address the problem of uniform illumination of all photocatalytic particles and exploits catalyst particles adapted to the constraints imposed by the reactor.

Parameters that are important to all reactor design include [4] (i) mode of operation, (ii) phases present, (iii) flow characteristics, (iv) heat exchange requirements, and (v) composition and operating conditions of the reaction mixture. The requirement for photons as a reactant imposes additional considerations. There are six common ways to deliver light as listed here. (a) *Immersion wells* have one or more lamps that are immersed in a well-stirred reactor. This is mainly used in the laboratory. (b) *Multilamp reactors* have a cylinder surrounded externally by several lamps and a reflector. (c) it Elliptical reactors have lamps at the foci that are mounted vertically. (d) *Film type* reactors have a thin film of liquid flowing over an externally irradiated wall. (e) *Flat walls reactors* are used when the light beam is parallel. A transparent wall of the reactor is usually flat and the sample can flow co-current, counter current, or cross. (f) *Annular photoreactors* have two co-axial cylinders that define the reaction zone. A lamp is usually placed on the axis. In this arrangement, the light is absorbed by the reactive system in the annular region. This type of arrangement is often used in industrial UV applications [5].

1.1. *Fluidized bed reactor designs*

The purpose of this paper is to present a solution to requirements of a photocatalytic reactor for aqueous streams that can combine substrate pre-concentration. The annular design (f) and the cylindrical system with multi-lamp arrangements (b) are exploited in the designs described. The objective was to fluidize the photocatalyst in the annular/cylindrical region. The fluidized bed approach was chosen in an attempt to ensure that all photocatalytic particles receive uniform illumination. The empirical demonstration that uniform illumination can be achieved is reviewed below. A second-generation lab reactor (reactor volume = 7 l) is the tool for evaluation of several parameters of performance reported here. It was designed to incorporate two ways of light delivery: the annular design with a central lamp and the multi-lamp setup on the perimeter of the reaction zone. A small pilot scale reactor (36 l) has been fabricated following a more conventional (for industrial applications) annular design. It was preliminarily tested on a pilot line at the Bearspaw water treatment plant of Calgary Waterworks Division. Its performance is compared to the lab reactor.

1.2. *Integrated photocatalyst adsorbent (IPCA) and the "golf ball" concept*

Fine TiO_2 powders present separation problems in slurry type reactors leading to complications and expense. As a result, a number of efforts have been made to support TiO_2 on fixed or mechanically manageable supports. In a fluidized bed reactor, the particle size must be larger than the low micron size range of TiO_2 powders for retention of the solids in the reactor. In our case, the interest is in TiO_2 supported on an adsorbent high silica zeolite, i.e., an integrated photocatalytic adsorbent (IPCA). This combination alone is a fine powder and is not of high mechanical stability so that it is subject to attrition. That has led to adoption of a porous carrier for the TiO_2–zeolite combination in a configuration called the "golf ball" concept. According to this idea, the integrated photocatalyst adsorbent (IPCA), a composite of TiO_2 and a zeolite (as the adsorbent) is impregnated into the caverns of sintered porous glass beads. The purpose of the sintered glass beads (SIRAN^{TM}, Jeager Biotech Engineering) with pore diameters up to 120 μm was to provide channels (imagined as similar to the dimples of a golf ball) into which TiO_2 (approx. 20 μm) and zeolite (approx. 40 μm) could penetrate for protection from mechanical attrition during fluidization.

In the process of synthesizing the initial IPCA material, Degussa P-25 TiO_2 and Silicalite I (S-115, Zeolyst International) were attached directly to the glass beads by mixing the components into a slurry in 40% colloidal silica binder. Laboratory scale evaluation of such an IPCA has been reported and the process optimized [3]. Larger quantities are required for experiments in the photoreactors described here and the current preparation is given in the experimental section. Figure 1(a) and (b) show electron micrographs of the original beads and the beads after loading. The occupation of "dimples" is seen.

Mechanical stability of IPCA (how well the IPCA components are retained) was assessed by tumbling the IPCA material in water on a roller for a period of 1 month. Such conditions were supposed to simulate the effect of attrition happening during fluidization in the photoreactor. To aggravate the attrition conditions, steel nuts were added to the second trial bottle containing IPCA. Adsorption capacity, photoactivity and particle size distribution of IPCA were then compared to the initial values. None of the monitored characteristic seemed to be affected by the simulated attrition, which led to the conclusion that the IPCA material was made mechanically robust. Consecutive multiple trials in the photoreactor did not affect IPCA activity either.

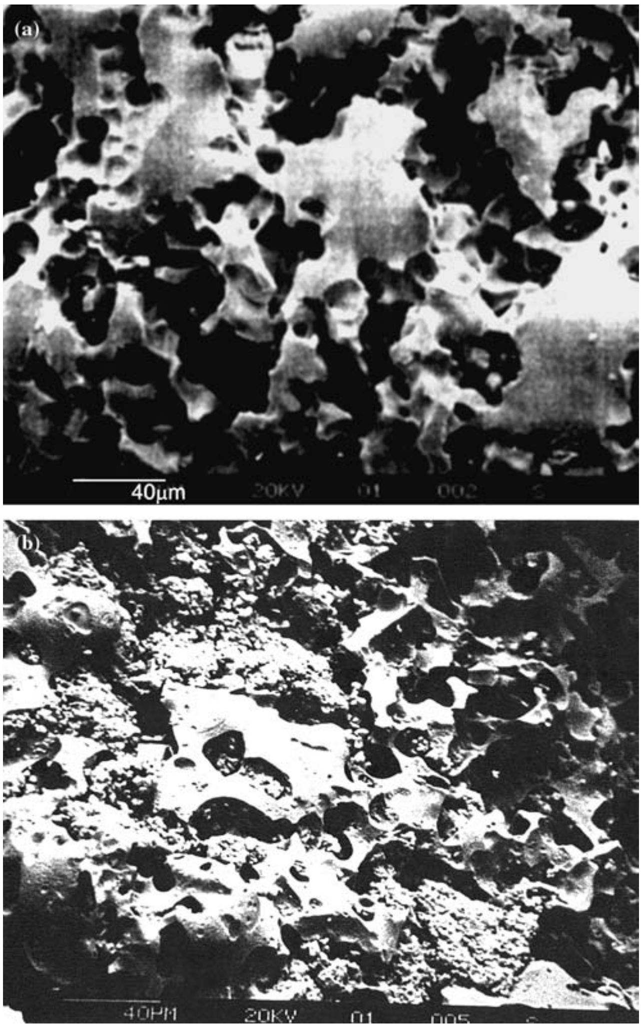

Fig. 1. SEM images of (a) porous glass beads and (b) titania and zeolite loaded on the beads.

1.3. *Fluidization imaging*

For heterogeneous photoreactions, the contact between photons and particles must be maintained uniform and maximized. For liquid–solid systems and gas–solid systems, stirred tank or fluidized bed photo-reactors are to be preferred despite cost and operational delicacy. To test fluidization of IPCAs and the adsorption properties of the IPCA, a dual mode fixed bed-fluidized bed reactor with full recirculation was constructed [6]. The design is very similar to that of the lab reactor shown in Figure 2. Key dimensions of this reactor were as follows: height: 81 cm, reaction zone: 20 cm, lamp enclosure: 7 cm. Cooling water enters the bottom and exits the top of the inner chamber. The reaction system is in the annulus with fluidization flow from the bottom and an option for flow from the top to study adsorption by the IPCA as a fixed bed. The enclosures are quartz

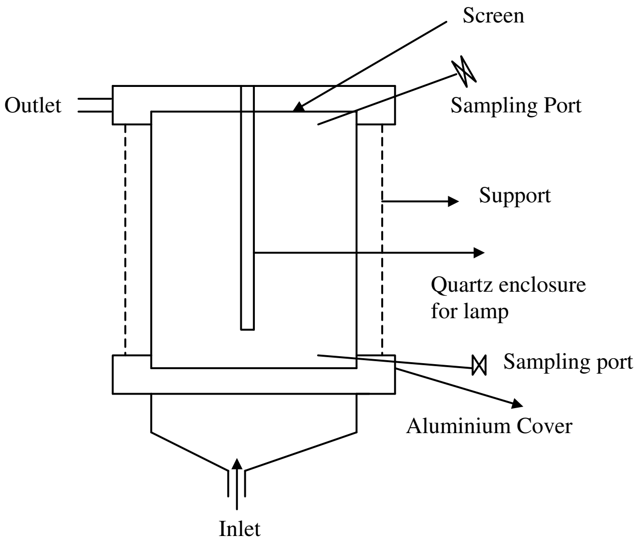

Fig. 2. Schematic diagram of the second-generation lab reactor.

glass to permit transmission of UV. Loss of particles at the top is prevented by a 425 μm nylon mesh screen held between Plexiglas plates with 58 holes of 5 mm diameter. A similar structure is at the bottom.

Fluidization was studied by particle tracking using both CAT scanning and radioactive particle tracking. CAT scanning experiments were conducted using a fourth generation X-ray CAT scanner (EMI 7070) modified to scan vertically oriented objects. With spatial resolution as low as 0.2 × 0.2 mm and temporal resolution as low as 2 s. Data was acquired by scanning the bed using a 1 cm slice. The algorithms and data analysis were as used earlier [7, 8]. Radioactive tracking for 3-D images was conducted with two gamma cameras set-up at right angles started simultaneously manually. Images were synchronized by finding a time lag between the cameras using auto-correlation. Images were obtained at 5 Hz. Photocatalysts were tagged with Technetium macroaggregated albumin (^{99m}Tc-MAA). The cameras had a circular field of view of 41 cm diameter that was imaged at 128 × 128 pixels giving a resolution of 3.2 mm in particle location. Images were obtained at 20 Hz.

The CAT scans allowed development of a detailed picture of the effects of flow velocity on distributions. At sufficient velocity, voidage maps show disappearance of distributor effect and smooth and uniform fluidization can be inferred. This is verified directly by the gamma tracking maps. Figure 3 [6] shows particle positioning in the prototype photoreactor at a superficial velocity of 0.66 cm s^{-1}. Thus, it was demonstrated that a uniform illumination of the IPCA is possible under reasonable conditions. During those experiments, the outer envelope was replaced with Plexiglas to avoid gamma attenuation.

2. Experimental section

2.1. *Materials*

Titanium dioxide (P25 grade) was a gift from Degussa Corporation; zeolite Silicalite I (S-115) was purchased from Zeolyst International; porous glass beads (SIRAN^{TM} carriers) were purchased from JAEGER Biotech Engineering Inc.; colloidal silica (40 wt% silica suspension in water) and phenol were purchased from Aldrich and used as received.

The IPCA material was manufactured on a larger scale (up to 10 kg) for the purpose of using it in the second-generation lab reactor (7 l) and small-scale pilot reactor (36 1). The manufacturing process was based on the prior laboratory optimization [3], which involved pre-treatment procedures and modification of the ratio of the components in order to achieve better catalyst stability and resistance to attrition under fluidization conditions. A prior loading of TiO_2 onto the zeolite was the first stage of the manufacturing process and was performed before attaching the components to the porous glass beads (pre-treatment). Pre-treatment of titania and zeolite powders involved sonication and calcination procedures where the two active components were first slurried together in water, sonicated, dried at 120 °C, and then heated at 450 °C. This led to firm attachment of TiO_2 to the zeolite. Sonication was done in an Aquasonic bath (model P250D) at 60 °C for 1 h. Thermal pre-treatment of the components was done in a muffle furnace (Hotpack Inc.) for 8–12 h.

Elsewhere, ^{29}Si CP MAS solid state NMR has demonstrated that firm titania–zeolite attachment

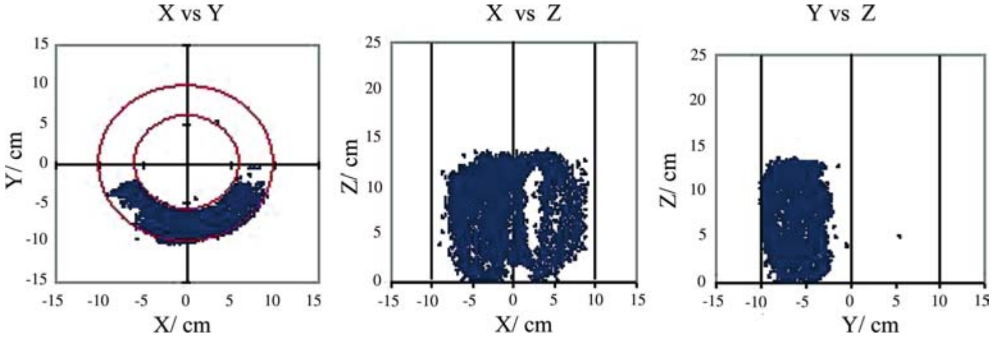

Fig. 3. Particle positioning in the prototype photoreactor at a superficial velocity of 0.66 cm s^{-1} [6].

occurs via Si–O–Ti bonds replacing surface Si–O–H groups [9, 10]. ^{29}Si NMR and XRD [9] showed that larger than 5 wt.% TiO_2 loading lead to the growth of longer anatase crystallites with little increase of zeolite surface coverage above the ~23% achieved at 2.5 and 5.0 wt.% coverage by TiO_2.

In the next stage of the manufacturing of IPCA, the combined TiO_2/zeolite particles were bound to the glass beads as described in [3]. The following composition – beads: P25: Silicalite I: silica gel = 73:1:3:23 was used for the preparation of the improved IPCA material intended for piloting. This sample has five times lower loading of the active components (titania and zeolite) onto the support as compared to the initial [3] composition of the IPCA material originally synthesized for the lab use. The change substantially reduces attrition. This happens at the expense of reduced adsorption capacity. Comparison of the performance of the initial IPCA material originally prepared for the lab experiments and the later improved version of the IPCA material prepared for the pilot scale experiments in the same (lab) reactor shows that they display nearly indistinguishable photochemical performance.

2.2. *Design of fluidized bed photoreactors and experimental procedures*

A second-generation lab reactor with the holding capacity of 7 l was constructed based on co-axial cylindrical geometry with an external multi-lamp arrangement. The geometry of the reactor allowed the option of inserting an additional UV lamp on the axis. The cylinders were fabricated from quartz to allow maximum UV transmission into the reaction zone from inside and outside. Top and bottom parts of the reactor were made from anodized aluminum. The bottom portion of the reactor is conical to allow water to enter as a jet and then be distributed through the distributor. The photocatalyst particles are retained by 425 μm nylon mesh screen held between steel plates with 58 holes of 5 mm diameter. An external multi-lamp arrangement is provided by a Rayonet [New England Nuclear] lamp system enclosed by a reflector. There are two sampling ports at the top and bottom of the reactor to collect samples for analysis. Detailed design of the second-generation lab reactor and its positioning within the Rayonet multiple lamp arrangement are shown on Figures 2 and 4, respectively.

A small pilot scale reactor based on the annular geometry was constructed by scaling up the prototype photoreactor described in the introduction section. The reactor height, outer and inner diameters are 1.025 m, 0.256 m and 0.144 m, respectively and its holding capacity is 36 l. The outer cylinder was made of aluminum and the inner cylinder was made of quartz. Four UV lamps (254 nm wavelength) were placed inside the inner cylinder. The annular portion of the reactor was filled with certain amount of the catalyst that was fluidized by circulating contaminated water through the reactor. The distributor plate was made of two circular aluminum plates with 58 holes of 5 mm diameter each arranged in a triangular pitch and had a Nylon screen of 425-micron-size sandwiched in between, in order to prevent the back-flushing of photocatalyst particles.

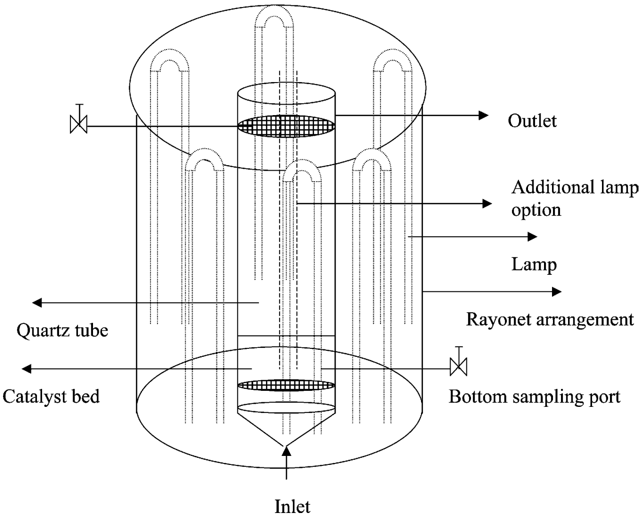

Fig. 4. Schematic diagram of the second-generation lab reactor within the Rayonet multiple lamp setup (dimensions: lamp height: 44 cm, Rayonet height from bottom: 53 cm, number of lamps: 8, lamp diameter: 3.2 cm, lamp-to-quartz tube distance: 10~12 cm).

The complete system setup consists of the photoreactor (lab or pilot scale) and water re-circulation line that includes a pump and tank for facilitating the storage of water for use during regeneration as shown on Figure 5. The flow path of the reactor is 1-2-3-4-1, as marked in the figure. Total system volume is 59 l for the lab reactor and 100 l for the pilot reactor. The rotameter in the left corner and the pipe and hose line associated with it are for an alternative source of water supply. The pump

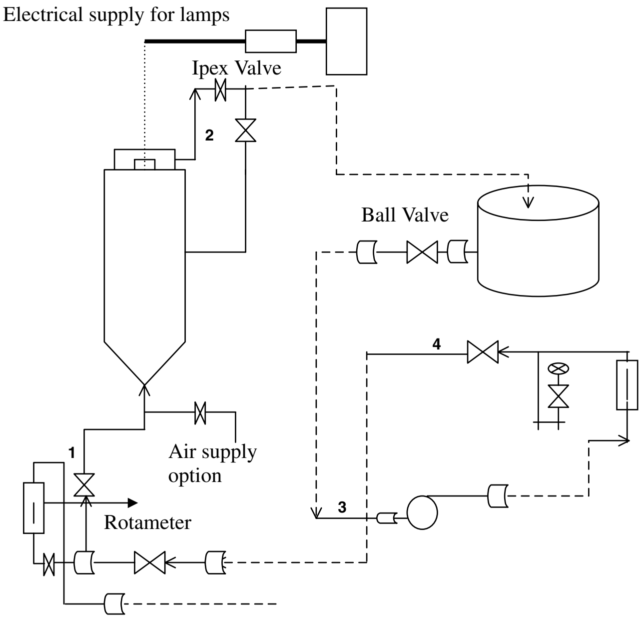

Fig. 5. Schematic diagram of the complete system setup including the flow arrangement.

used is a Goulds NPE, 90 V, 3.5 A, close coupled, end suction, single stage centrifugal pump with flow regulator. A number of Cole Palmer flowmeters of different ranges are used in order to measure the water flowrate at the input and output of the reactor. A pressure gauge has been installed to keep track of pressure build-up in the reactor in the event of screen clogging due to fines generation during the process. All the connections from the pump to the photoreactor and tank are of flexible Tygon hoses.

Phenol was used as a model pollutant in this series of experiments. Initially, a certain amount of phenol was introduced in the storage tank and then passed through the reactor for an hour in the dark to allow for saturation of the IPCA material. Afterwards, the lamps were turned on and a straight recycle process was initiated (no new phenol was added to the system). The process of phenol degradation was monitored using HPLC. The instrument had a C_{18} column operated under the following conditions: the wavelength of the UV detector was set at 224 nm; a 50:50 mixture of CH_3CN and H_2O was used as an effluent with 1.0 ml min^{-1} flow rate. Analytical results were calibrated using a series of standard solutions corresponding to a range of concentrations used in the experiments. Reactor light intensities were measured by ferrioxalate actinometry [11].

3. Results

3.1. *Optimization of operational parameters*

The major objective of this part of research was to determine a range of favorable operating parameters and overall behavior of the photocatalyst in the second-generation lab reactor so that it can be transferred to the larger scale pilot reactor. In this section, effects of certain operational parameters, such as IPCA loading, light distribution, and addition of H_2O_2, are presented. Characterization of the photocatalyst involved determination of a minimum fluidization velocity and terminal velocity and optimization of particle size distribution suitable for fluidization in the reactor.

Minimum fluidization and terminal settling velocity calculations were performed based on the Ergun equation [12]. The calculated minimum fluidization velocity is equal to 0.58 cm s^{-1} and terminal velocity is 8.3 cm s^{-1}. In volumetric units, these values correspond to 5.7 l min^{-1} and 81 l min^{-1}, respectively for the lab reactor and 12 l min^{-1} and 175 l min^{-1}, respectively for the pilot reactor. Experimentally, the flow rate was 27 l min^{-1} in the lab reactor and 46 l min^{-1} in the pilot reactor.

The initial particle size distribution of the carrier beads and the IPCA material was in the range of 0.4–1 mm diameter. During fluidization in the reactor, smaller size particles of the IPCA material were clogging the mesh screens, which in turn led to a drop in the operating pressure in the system and suboptimal fluidization. In order to avoid obstruction of water flow, a fluidization method to remove small particles was adopted. The upper screen was omitted allowing some particles to overflow. This eliminated the portion of the particles potentially causing the clogging. Thus, a portion smaller than 0.6 mm was removed from the reactor and a range of 0.6–1 mm remained.

Optimization of IPCA loading in the reactor is important from the point of view of maximized light delivery to the catalyst. Both insufficient and overestimated loadings would lead to inefficient degradation rate. As shown on Figure 6, 200 g (0.21 g l^{-1} Titania) loading leads to low degradation of the test compound, as did 2.0 kg (2.14 g l^{-1} Titania) loading. Optimum catalyst loading was indicated to be in the range of 1.0 kg (1.07 g l^{-1} Titania)–1.5 kg (1.61 g l^{-1} Titania) of the IPCA material. The upper end of this range defines the upper end of the adsorption capacity provided by the zeolite load.

In order to address the issue of light distribution in the reaction zone, the effect of UV light positioning inside the reactor was investigated in the lab version of the photoreactor. Before commencing irradiation experiments, it was necessary to evaluate the absolute light intensity of the irradiation. Chemical actinometry was used to measure the light intensity. The commonly used potassium ferrioxalate system $K_3[Fe^{III}(C_2O_4)_3]\cdot 3H_2O$ was adopted and used as described by Calvert and Pitts [11]. It has good sensitivity for wavelengths from 254 nm to 480 nm. Experimentally, it was found that the UV intensities were 5.1×10^{17} photons s^{-1} and 9.0×10^{18} photons s^{-1} for the inner and outer lamps in the lab reactor, respectively. In the pilot reactor, the intensity of the lamps was 3.2×10^{17} photons s^{-1}. Results of the degradation experiments with the inner and outer lamp positioning are shown in Figure 7 with higher conversion observed with the outer lamps. However at high light intensity, degradation rate on

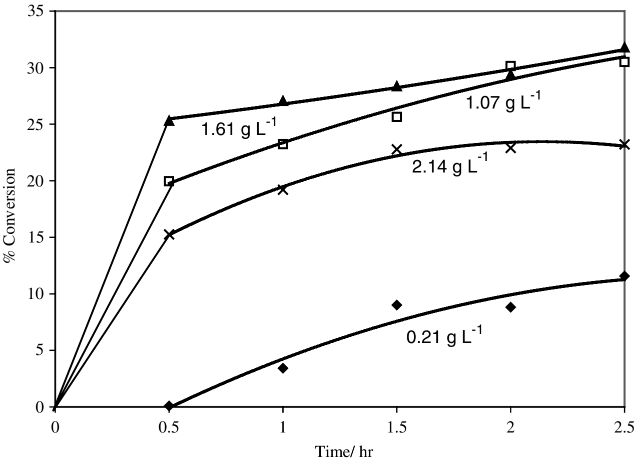

Fig. 6. Optimization of IPCA loading in the second-generation lab reactor (flow rate: 27 LPM; all lamps on). There is no theoretical base for the functions. Trend lines are to aid visualization only.

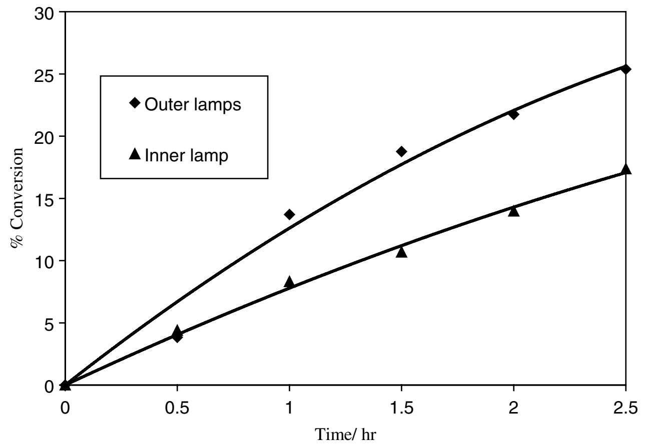

Fig. 7. Effect of UV light distribution (titania loading: 1.07 g l^{-1}, flow rate: 27 l min^{-1}). Trend lines are only an aid to visualization.

TiO$_2$ varies as the square root of light intensity [13]. Normalization to the corresponding light intensities, indicates that the annular design is superior by approximately a factor of two. The surface area through which the light enters is, of course larger at the outer wall. The actinometer solution is free of particles and produces little light scattering. However, the particulate catalyst scatters efficiently and will be associated with large losses by scattering back out of the reaction chamber through the larger area outer wall.

3.2. *A role for H_2O_2*

It was found in a number of phenol experiments that dimers and/or higher polymeric compounds are formed, as indicated by appearance of pink color within minutes of irradiation. This was verified by UV spectra where the phenol peak broadened and decreased in height. In this circumstance, total organic carbon (TOC) values drop initially but reach a steady state and show virtually no reduction afterwards. The problem is probably a consequence of local concentrating of phenols on the zeolite adsorbent so that radical coupling is favored since it is not observed on TiO$_2$ alone. In some cases increasing electron capture by addition of H_2O_2 accelerates degradation of organics [14] and can overcome deactivation due to accumulation of less degradable reaction byproducts [15]. One percent of the stoichiometrically required H_2O_2 was added simultaneously with initiation of irradiation or 1 h later. Only H_2O_2 added at initiation of the irradiation overcame dimerization. As shown in Figure 8, a small addition of H_2O_2 added only at the initiation of the reaction accelerated photooxidation by a factor of two. The stoichiometrically low level of H_2O_2 is insufficient to regard it as a replacement for O_2 as the primary electron acceptor from the TiO$_2$ conduction band or as a main source of $^{\bullet}$OH radical. Its function must be establishment of a radical mechanism favorable to faster degradation.

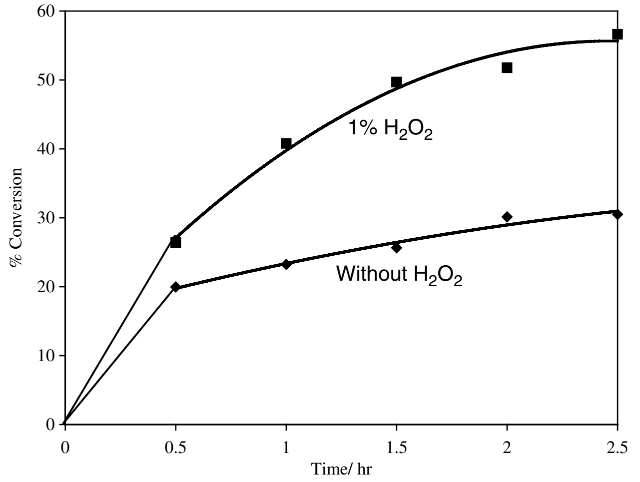

Fig. 8. Effect of H_2O_2 addition (titania loading: 1.07 g l^{-1}; all lamps on; flow rate: 27 l min^{-1}). Trend lines are only an aid to visualization.

3.3. *Photocatalyst "poisoning"*

It was found that the photocatalytic activity of the IPCA was significantly reduced during long term use (Figure 9) similarly to other reports [16]. Acid-wash and calcination treatments were evaluated for catalyst re-activation with the expectation that the former would remove inorganic deposits and the latter ash organic films. The acid-wash was performed by mixing with 0.5 M HCl solution at a weight ratio of 1:20 (solid:acid) and heating with stirring for 1 h in the 85–95 °C temperature range. Calcination was done at 400 °C for 4 h.

It appeared that acid-wash procedure completely regenerated poisoned catalyst, while calcination was not effective. This implies that the loss of catalyst activity can be attributed to the accumulation of inorganics such as (especially) iron oxides and not to organic by-product films.

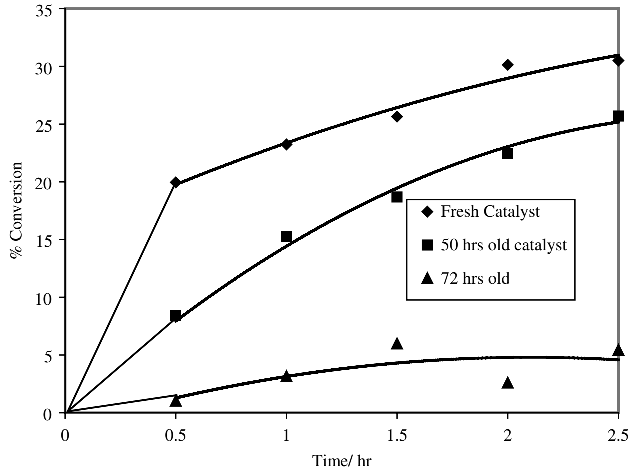

Fig. 9. Decrease of IPCA activity over time (poisioning) (titania loading: 1.07 g l^{-1}; all lamps on, flow rate: 27 l min^{-1}). Trend lines are only an aid to visualization.

3.4. *Trial of the pilot photoreactor at Bearspaw water treatment plant*

The composition of the IPCA material for the first testing of the photoreactor at the Bearspaw Water Treatment plant was the same as in the lab trials. The photoreactor was loaded with 3 kg of IPCA (0.55 g l^{-1} Titania). During the first stage saturation, phenol was allowed to flow from the top to the bottom of the reactor and pass through the fixed IPCA bed where it was adsorbed by the zeolite from the IPCA material. The flow rate was chosen as 2 l min^{-1} to achieve slow and uniform saturation of IPCA. The concentration of phenol in the effluent was monitored during the saturation process as shown in Table 1. Breakthrough begins to become significant before 1 h. IPCA assisted phenol photolysis was performed at a 46 l min^{-1} flow rate and the results are shown in Figure 10.

4. Conclusions

The lab and pilot trials to date demonstrate that it is feasible to prepare an IPCA of sufficient mechanical resilience to allow for use of the fluidized bed approach as the means to ensure uniform photocatalyst illumination by exploitation of the "golf-ball" concept. Pre-concentration can be achieved by reverse flow of contaminated solution through the IPCA as a fixed bed. The most effective geometry for illumination appears to be the annular type design. A surprising result arising from the choice of phenol as a test compound is the observation that an initial and sub-stoichiometric H_2O_2 addition has a significant accelerating effect. The radical chain mechanism responsible for the sub-stoichiometric effect remains to be elucidated. It must be emphasized that the performance of the present reactors is limited by the lamp arrangements that were available in consequence of electrical infrastructure. Use of state of the art lamp systems could greatly enhance performance.

Table 1. Monitoring the saturation process of 3 kg IPCA with 13-ppm phenol solution

Time of saturation/min	15′	30′	60′	90′	120′	150′	180′
Phenol concentration in the effluent/ppm	2	2	4	7.4	12	12.8	13.3

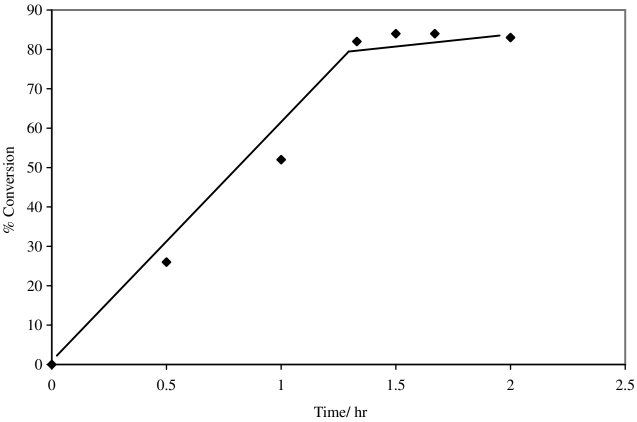

Fig. 10. Preliminary experiment with the pilot photoreactor at the Bearspaw water treatment plant. Trend lines are only an aid to visualization.

References

1. Y. Xu and C. Langford, *J. Phys. Chem. B* **101** (1997) 3115.
2. J. Chen, L. Eberlein and C.H. Langford, *J. Photochem. Photobiol. A: Chem.* **5994** (2002) 1.
3. F. Haque, E. Vaisman, C.H. Langford and A. Kantzas, *J. Photochem. Photobiol. A: Chem.* **169** (2004) 21.
4. V. Augugliaro, V. Loddo and M. Schiavello. Heterogeneous photocatalytic reactors: An assessment of fundamental engineering aspects, *in* M. Schiavello (Ed), Heterogeneous Photocatalysis, (John Wiley and Sons, NY, 1997), pp. 169.
5. A.M. Braun, L. Jakob and E. Oliveros, *Adv. Photochem.* **18** (1993) 235.
6. A. Bhargava, M.F. Kabir, E. Vaisman, C.H. Langford and A. Kantzas, *J. Ind. Eng. Chem. Res.* **43** (2004) 980.
7. A. Kantzas, I. Wright and N. Kalogerakis, *Chem. Eng. Sci.* **52** (1997) 2023.
8. A. Kantzas and N. Kalogerakis, *Chem. Eng. Sci.* **51** (1996) 1979.
9. E. Vaisman, R.L. Cook and C.H. Langford, *J. Phys. Chem. B* **104** (2000) 8679.
10. Y. Chang, *M.Sc. thesis*, University of Calgary. (2004).
11. J.G. Calvert and J.N. Pitts Jr., 'Photochemistry' (John Wiley & Sons, Inc., 1966), p. 783.
12. Y.G. Yates, *Fundamentals of Fluidized-bed Chemical Processes* (Butterworths Monographs in Chemical Engineering, U.K., 1983), pp. 5.
13. D.F. Ollis, E. Pelizzetti and N. Serpone, *Environ. Sci. Technol.* **25** (1991) 1523.
14. D.D. Dionysiou, M.T. Suidana, I. Baudinb and J.M. Laînéb, *Appl. Catal. B: Environ* **50** (2004) 259.
15. S.A. Larson and J.L. Falconer, *Appl. Catal. B: Environ.* **4** (1994) 325.
16. K.V. Subba Rao, M. Subrahmanyam and P. Boule, *Appl. Catal. B: Environ.* **49** (2004) 239.